Check for updates

ADVANCED OPTICAL MATERIALS
www.advopticalmat.de

Optical Activity and Phase Transformations in γ/β Ga_2O_3 Bilayers Under Annealing

Alexander Azarov, Augustinas Galeckas, Ildikó Cora, Zsolt Fogarassy, Vishnukanthan Venkatachalapathy, Eduard Monakhov, and Andrej Kuznetsov**

Gallium oxide (Ga_2O_3) can be crystallized in several polymorphs exhibiting different physical properties. In this work, polymorphic structures consisting of the cubic defective spinel (γ) film on the top of the monoclinic (β) substrate are fabricated by disorder-induced ordering, known to be a practical way to stack these polymorphs together. Such bilayer structures are annealed to investigate optical properties and phase transformations. Specifically, photoluminescence and diffuse reflectance spectroscopy are combined with transmission electron microscopy, Rutherford backscattering/channeling spectrometry and X-ray diffraction to monitor the evolutions. As a result, a two-stage annealing kinetics is observed in γ/β Ga_2O_3 bilayers associated with the epitaxial γ-to-β regrowth at the interface at temperatures below 700 °C and a non-planar γ-to-β phase transformation starting at higher temperatures. Thus, the present data enhance understanding of the polymorphism in Ga_2O_3, interconnecting the phase transformation kinetics with the evolution of the optical properties.

1. Introduction

Ultra-wide bandgap semiconductors, such as gallium oxide (Ga_2O_3), have attracted unprecedented research interest during the past decade.[1] Such attention is stimulated by their unique material properties offering numerous potential applications, e.g. in power electronics and optoelectronic devices capable of operating in the deep UV spectral range.[2–5] Equally importantly, Ga_2O_3 can be crystallized in several polymorphs having different structures[6–9] and, consequently, physical properties. The monoclinic (β) Ga_2O_3 phase is thermodynamically stable at normal conditions, while the rhombohedral (α), defective spinel cubic (γ), orthorhombic (κ), and bixbyite-like cubic (δ) phases are metastable.[6–9] As such polymorphism of Ga_2O_3 may provide additional functionalization opportunities;[10] for example, if fabricating bilayer consisting of different polymorphs.

According to thermodynamics, polymorphism is a function of temperature and pressure. However, recently it was demonstrated that β-to-γ phase transitions in Ga_2O_3 can be governed by the disorder-induced ordering during ion bombardment.[11–13] Spectacularly, this transition occurs after reaching the disorder threshold[14] resulting in the formation of the γ/β double layer structure having an abrupt interface. Notably, such structures exhibited remarkably high radiation tolerance, limited primarily by the stoichiometric lattice distortions due to incorporation of the implanted ions.[13] The perspective of using γ-Ga_2O_3 for radiation tolerant devices was recently tested in the corresponding Schottky diodes.[15]

The present study aims to investigate optical properties in such γ/β Ga_2O_3 bilayers as a function of the annealing temperature, in correlation with the polymorph transition monitoring; not least because there are only few initial studies of the γ-Ga_2O_3 thermal stability reported in literature.[16–20] In our work, we observed a distinct two-stage annealing kinetics in γ/β Ga_2O_3 bilayers associated with the epitaxial γ-to-β regrowth at the interface at temperatures below 700 °C and a non-planar γ-to-β phase transformation starting at higher temperatures. This novel observation enhances understanding of the polymorphism in Ga_2O_3, interconnecting the phase transformation with the evolution of the functional properties.

2. Results and Discussion

Figure 1a,b illustrates structural evolutions occurring in γ/β double layer structures during annealing, showing the Rutherford backscattering spectrometry in channeling mode (RBS/C) spectra and corresponding X-ray diffraction (XRD) 2Θ scans, respectively. For the as-fabricated sample, the RBS/C spectrum

A. Azarov, A. Galeckas, V. Venkatachalapathy, E. Monakhov, A. Kuznetsov
Department of Physics
Centre for Materials Science and Nanotechnology
University of Oslo
PO Box 1048 Blindern, Oslo N-0316, Norway
E-mail: alexander.azarov@smn.uio.no; andrej.kuznetsov@fys.uio.no
I. Cora, Z. Fogarassy
HUN-REN Centre for Energy Research
Institute of Technical Physics and Materials Science
Konkoly-Thege M. u. 29–33, Budapest 1121, Hungary
The ORCID identification number(s) for the author(s) of this article can be found under https://doi.org/10.1002/adom.202401325

© 2024 The Author(s). Advanced Optical Materials published by Wiley-VCH GmbH. This is an open access article under the terms of the Creative Commons Attribution-NonCommercial-NoDerivs License, which permits use and distribution in any medium, provided the original work is properly cited, the use is non-commercial and no modifications or adaptations are made.

DOI: 10.1002/adom.202401325

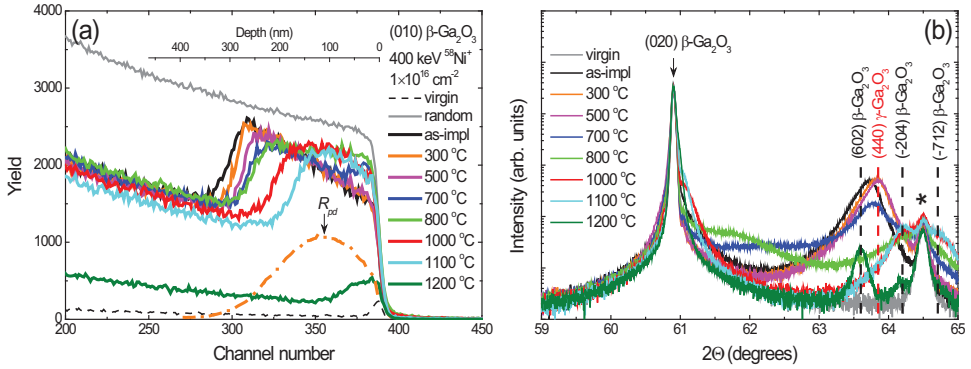

Figure 1. Systematic structural analysis of γ/β bilayer anneals. (a) RBS/C spectra and (b) corresponding XRD 2Θ scans of γ/β Ga_2O_3 bilayers before and after annealing as indicated in the legends. The peak marked by star in the panel (b) is because of the sample holder. The RBS/C and XRD spectra of the unimplanted (virgin) β-Ga_2O_3 samples are also included in the corresponding panels for comparison. Dashed-dotted line in panel (a) illustrates the nuclear energy loss versus depth profile calculated with SRIM code;[22] the arrow indicates the maximum stopping power (R_{pd}) position.

exhibits a characteristic box-like shape "inclined" toward the surface, known as a fingerprint of the crystalline γ-Ga_2O_3 film on top of β-Ga_2O_3 substrate.[13] Such bilayer state of the initial sample is further confirmed by the XRD data showing both the (020) β-Ga_2O_3 reflection and the (440) γ-Ga_2O_3 peak centered at ≈63.75° in good agreement with the literature value of 63.85°.[21] Notably, the as-fabricated γ film is ≈300 nm thick. However, this thickness decreases in the course of anneals as clearly seen from the gradual narrowing of the RBS/C box-like signature. For example, upon 500 °C anneal, its thickness decreases to ≈275 nm, see Figure 1a. This reduction of the γ layer thickness may be interpreted as γ-to-β polymorph regrowth from the initial interface toward the surface. At the same time, the γ-phase XRD peak moves closer to the tabulated position of the (440) γ-Ga_2O_3 planes indicating structural improvements, see Figure 1b.

However, for anneals at ≥700 °C this trend is interrupted and new features are observed in Figure 1. Indeed, as seen from Figure 1a, upon 700 °C anneal the channeling yield increases near the surface as compared to that in the samples annealed at lower temperatures. This behavior correlates with a significant decrease in the amplitude of the γ-related XRD peak and also accompanied with the enhancement of the background intensity between the (020) β- and (440) γ-Ga_2O_3 reflections. Further, upon 800 °C anneal the (440) γ-Ga_2O_3 peak vanishes, see Figure 1b. Instead, new XRD peaks centered at ≈64.2° and ≈64.7° emerge; which can be assigned to the (−204) and (−712) reflections in β-Ga_2O_3,[23] indicating misoriented reconstruction in respect with the initial wafer orientation. Thus, this new trend may be interpreted as γ-to-β transformation resulting in differently oriented β-phase regions forming in the vicinity of the surface, in correlation with the RBS/C data. Further on, anneals at 1000 and 1100 °C, lead toward even better definition of the (−204) and (−712) β-Ga_2O_3 XRD peaks; again in correlation with the corresponding RBS/C data showing higher dechanneling yield, as such confirming the hypothesis of the β-phase misorientation. In contrast, upon 1200 °C anneal, the channeling is considerably improved, even though it still deviates from the virgin signal near the surface. The XRD 2Θ scan measured after 1200 °C anneal confirms further crystalline quality improvement; however, also detecting a new peak centered at 63.6° corresponding to the (602) β-Ga_2O_3 reflection,[23] in addition to the peaks at 64.2° and 64.7° (Figure 1b).

To verify the trends observed in Figure 1, the sample annealed at 1100 °C was selected for detailed transmission electron microscopy (TEM) study as summarized in **Figure 2**. Indeed, the bright field TEM image in Figure 2a shows that the sample consists of three distinct layers marked as Areas #1, #2 and #3. Area #1 corresponds to the initial β-Ga_2O_3 substrate. In Area #2, β-phase is epitaxial regrown in respect with the initial substrate orientation. In contrast, the near surface region labeled as Area #3 exhibits [200] "in plane" orientation (i.e., perpendicular to the initial [020]). Furthermore, in this region we observed twinning as seen from the fast Fourier transforms (FFTs) insets in Figure 2b taken from the corresponding areas as marked in the high resolution image in Figure 2b. In addition, it should be mentioned that the interface between Areas #2 and #3 is far from being abrupt. Thus, even though upon 1100 °C anneal the sample fully transforms back to the β-phase, the near surface misorientation results in the higher RBS/C signal as compared to that for the lower temperature anneals, see Figure 1a. Notably, these trends are not fully consistent with those observed during in situ anneals of similar γ/β structure performed in vacuum,[18] detecting the γ/β mixture already after 500 °C anneal; even though the β-phase misorientation was observed in the in situ anneals too.[18] The discrepancies in trends observed in our experiment and during in situ anneals may be attributed to the factors related to the annealing ambient and potentially different strain effects in macroscopic and TEM-lamella-sized samples. It should be noted that for γ-Ga_2O_3 films fabricated on different substrates the γ-to-β phase transformation can be also affected by a combination of strain and chemical effects related to the incorporation of such elements as Al and Mg migrating from the substrate during annealing[19,20] or additional chemical effects as recently suggested by Huang et al.[24]

At this end, under conditions of our experiment, we observe a distinct two-stage annealing kinetics in γ/β bilayered structures. The first stage occurs at temperatures <700 °C and is characterized by the shrinkage of the γ layer accompanied with the improvement of the γ-phase crystallinity. The second stage occurs at higher temperatures and is accompanied with the formation of the misoriented β-phase layer in the near-surface region. In the

© 2024 The Author(s). Advanced Optical Materials published by Wiley-VCH GmbH

21951071, 0, Downloaded from https://onlinelibrary.wiley.com/doi/10.1002/adom.202401325 by Hun-Ren Centre For Energy Research, Wiley Online Library on [08/09/2024]. See the Terms and Conditions (https://onlinelibrary.wiley.com/terms-and-conditions) on Wiley Online Library for rules of use; OA articles are governed by the applicable Creative Commons License

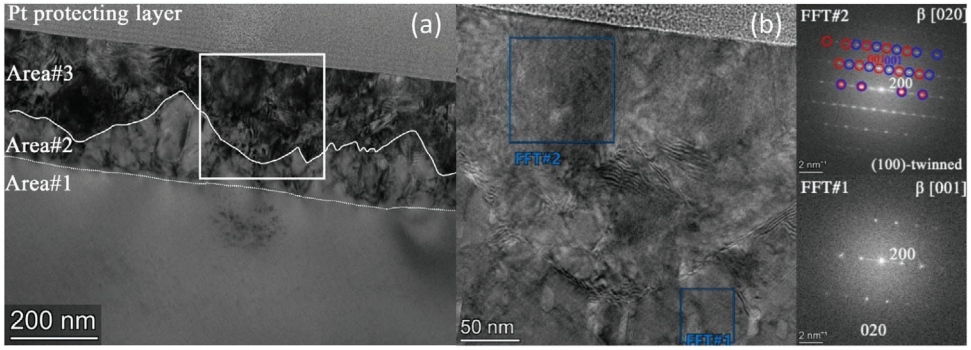

Figure 2. Detailed electron microscopy analysis of the sample annealed at 1100 °C. a) Bright field TEM image of the sample. b) High resolution TEM image of the area selected by white-colored frame in panel (a) together with the FFTs taken from the two different places in the sample as indicated by blue-colored frames in panel (b). Area #2 has the same orientation as the underlying (virgin) β substrate (i.e., Area# 1), while the reconstructed textured (twinned) β-phase is observed in the Area #3.

rest of the paper we study how this two-stage structural transformation correlates with optical properties.

Figure 3 summarizes optical absorption properties deduced from diffuse-reflectance spectroscopy (DRS) measurements carried out at room temperature (RT). First, Figure 3a,b represents selected raw data in semi-logarithmical and normalized scales, respectively. Two characteristic absorption onsets are observed in spectra of these samples, which is likely a signature of dissimilar optical band-edges for different light polarizations.[25] For clarity, in the Tauc plot analysis we consider the lowest onset as a representative of the optical bandgap, see Figure 3b. This procedure was systematically applied to all samples and Figure 3c summarizes the data. The trend observed in Figure 3c suggests that there is a threshold temperature range – indicated by a highlighted region in Figure 3c, beyond which the γ/β double layer structure is apparently converted into a single phase β-Ga_2O_3. This agrees well with a similar conclusion reached upon the analysis of the structural transformation trends in Figures 1,2.

Optical emission properties are summarized in **Figure 4**. Photoluminescence (PL) spectroscopy is known to be extremely sensitive to crystal quality modifications caused by irradiation and post-irradiation anneals.[26] Indeed, as seen from Figure 4 both the total quantum efficiency (QE) and the spectral response were affected in our samples. This is noticeable already from the raw data in Figure 4a, but is more apparent in Figure 4b, plotting the data normalized to the self-trapped hole (STH) emission centered at ≈3.2 eV. Indeed, changes in the green luminescence (GL) at ≈2.5 eV and red luminescence (RL) at ≈2 eV regions, are evident. In order to make more quantitative estimates, Figure 3c plots the results of the differential PL analysis of the corresponding shaded areas in Figure 4b. Thus, as clearly seen from the evolution of the total QE in Figure 4c, annealing leads to a gradual recovery of the crystallinity, also activating the defect-related RL band, which intensifies up to 800 °C and then rapidly turns off at higher temperatures. Such RL-band evolution may be readily correlated with the rearrangements occurring in the defective spinel structure as well as its transition to β-phase in agreement with the data in Figures 1 and 2.

For completeness of the PL data description, we admit that there is another prominent emission component centered at ≈694 nm (1.78 eV); as discussed in Supporting Information, this emission is related to Cr.[27] This spectral feature is because of Cr contamination artifact; however, prominent enough not to be ignored since it may strongly affect the optical performance.

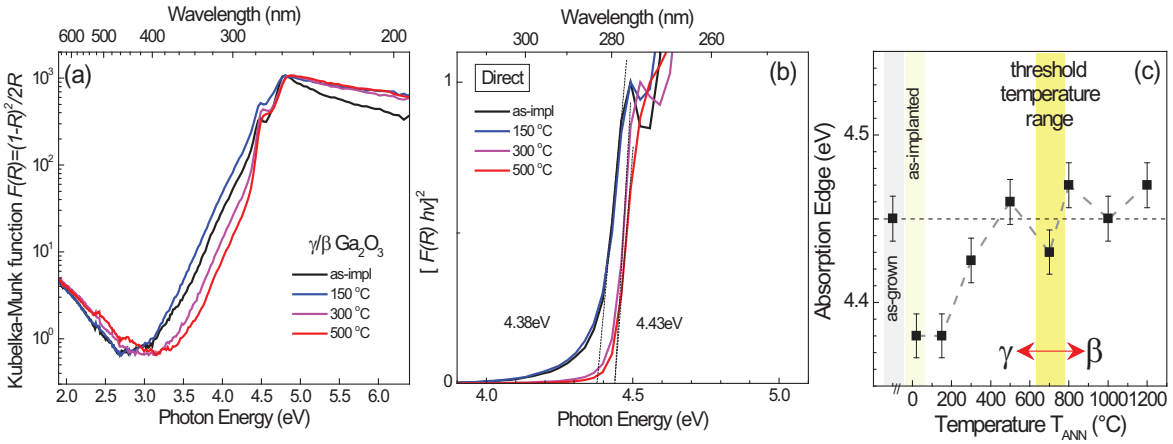

Figure 3. Evolution of the optical absorption in γ/β Ga_2O_3 bilayers as a function of annealing temperature, deduced from the DRS at 300K. a) Absorbance spectra for selected samples represented by Kubelka–Munk function $F(R)$. b) Corresponding Tauc plot for direct optical transitions; straight lines intersecting with the photon energy axis define the absorption-edge positions. c) Summary of the optical bandgap (absorption-edge) data.

© 2024 The Author(s). Advanced Optical Materials published by Wiley-VCH GmbH

21951071, 0, Downloaded from https://onlinelibrary.wiley.com/doi/10.1002/adom.202401325 by Hun-Ren Centre For Energy Research, Wiley Online Library on [08/09/2024]. See the Terms and Conditions (https://onlinelibrary.wiley.com/terms-and-conditions) on Wiley Online Library for rules of use; OA articles are governed by the applicable Creative Commons License

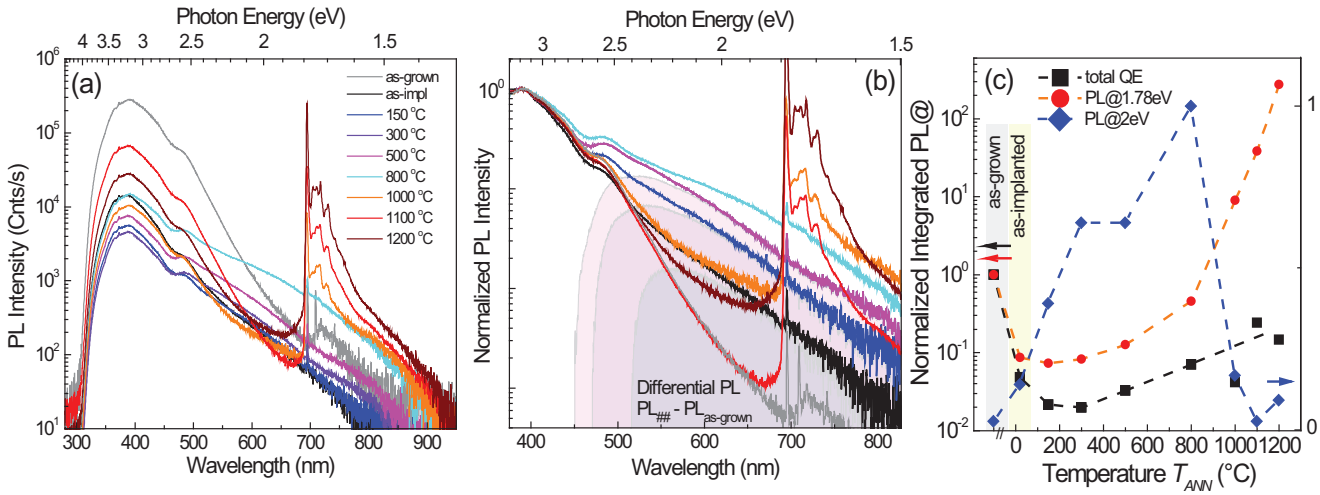

Figure 4. Evolution of the optical emission in γ/β Ga_2O_3 bilayers as a function of annealing temperature, deduced from PL spectroscopy at 10K. a) PL spectra as a function of annealing temperature. b) PL spectra normalized with regard to the intrinsic (excitonic) STH emission centered at 3.2 eV emphasizing the emission range associated with the implantation-induced defects. Shaded areas represent differential PL signatures obtained by subtracting emission of the unirradiated sample. c) Evolution of total QE, Cr^{3+} (R1/R2@1.78 eV) and defect-related emission (RL(@2 eV) as a function of annealing temperature. Note that total QE and Cr^{3+} evolutions are plotted on a semi-logarithmic scale (left-hand side axis), whereas defect-related intensities are on a linear scale (right-hand side axis).

3. Conclusion

In conclusion, we investigated the impacts of anneals on the phase transformations and corresponding optical response in γ/β Ga_2O_3 double layer structures initially fabricated by disorder-induced ordering. The results show that annealing kinetics of the γ/β Ga_2O_3 bilayer exhibits a distinct two-stage behavior associated with the epitaxial γ-to-β recrystallization at the interface at temperatures below 700 °C and a non-planar γ-to-β phase transformation at higher temperatures. Furthermore, non-planar transformations are accompanied with the β-phase misorientation in the near surface region. The optical properties are consistent with the structural transformations, both in terms of the γ-to-β bandgap switching and the evolution of the intrinsic defect emissions.

4. Experimental Section

In the present work, commercial (010) oriented β-Ga_2O_3 single crystals obtained from Tamura Corp were used. The γ/β Ga_2O_3 double layer structures were formed by means of RT bombardment with 400 keV $^{58}Ni^+$ ions to a dose of 1×10^{16} cm^{-2}. The ion irradiation was performed maintaining 7° off-angle orientation from normal direction to minimize channeling and the ion flux was kept constant at 5×10^{12} at/(cm^2s). This process is known to result in the γ/β double layer structure with an abrupt interface.[13] Subsequently, such γ/β bilayers were isochronically (30 min) annealed in the range of 150–1200 °C in air using a conventional tube furnace.

All samples were analyzed by a combination of the RBS/C, XRD, PL and DRS. In addition, selected samples were investigated by TEM. The RBS/C measurements were performed by 1.6 MeV He^+ ions incident along [010] direction in β-Ga_2O_3 part of the structure and backscattered into a detector placed at 165° relative to the incident beam direction. XRD 2Θ measurements were performed using the Bruker AXS D8 Discover diffractometer with high-resolution Cu $K_{\alpha1}$ radiation.

The highly contrasting thicknesses of γ and β phases in double layer structures (≈300 nm vs 300 µm, i.e., thickness ratio ≈1:1000) precludes the use of the most common approach in studying absorption, transmittance spectroscopy, where the signal is integrated over entire double layer structure making contribution from the relatively thin γ-phase layer indistinguishable from the dominating β-phase background. As an alternative, DRS technique is employed, which by a definition has an enhanced sensitivity to the near-to-surface material properties (due to evanescent light penetration, surface-roughness scattering, contrasting refraction in double layer structure, etc.). DRS measurements were carried out at RT using a UV-Vis spectrophotometer (Thermo Scientific, EVO600). The absorption spectra of the samples are represented by Kubelka-Munk function $F(R)$, which is equivalent of absorbance.[28]

PL spectra generally comprise emission components describing the intrinsic material properties and those introduced by ion irradiation and post-irradiation anneals. In Ga_2O_3 the intrinsic component is represented by the exciton related band, related to so-called STH.[29] The ion irradiation induced defects can provide non-radiative recombination pathways decreasing total QE, and/or introducing additional luminescent centers in PL spectra. The differential PL approach is used to visualize the implantation-induced defect contribution to emission spectra. This is done by subtracting spectrum of the non-implanted sample from all emission spectra. The photo-excitation at 246 nm wavelength (5.04 eV) and 10 mW average power was provided by a third-harmonic of the pulsed Ti:sapphire laser operating at 80 MHz in femtosecond mode-locked regime (Spectra-Physics, Tsunami HP and GWU-UHG-23). PL emission was collected by a microscope and analyzed by a fiber-optic spectrometer (Avantes, AvaSpec-Mini3648-UVI25) covering the wavelength range 200–1100 nm.

The TEM investigations were carried out in an aberration-corrected THEMIS microscope (THEMIS 200 TEM/STEM, Thermofisher Scientific/FEI) at 200 keV. Preparation of the cross-sectional TEM lamella was done in a SCIOS-2 type dual-beam FEG-SEM/FIB. TEM images and diffraction patterns were recorded at 200 keV with a 4k×4k CETA 16 CMOS camera. High resolution TEM images and corresponding FFTs were recordered from selected parts of samples too.

Supporting Information

Supporting Information is available from the Wiley Online Library or from the author.

© 2024 The Author(s). Advanced Optical Materials published by Wiley-VCH GmbH

21951071, 0, Downloaded from https://onlinelibrary.wiley.com/doi/10.1002/adom.202401325 by Hun-Ren Centre For Energy Research, Wiley Online Library on [08/09/2024]. See the Terms and Conditions (https://onlinelibrary.wiley.com/terms-and-conditions) on Wiley Online Library for rules of use; OA articles are governed by the applicable Creative Commons License

Acknowledgements

M-ERA.NET Program is acknowledged for financial support via GOFIB project (administrated by the Research Council of Norway project number 337627). A.A. and E.M. acknowledge the Research Centre for Sustainable Solar Cell Technology (FME SuSolTech, RCN project number 257639). The Research Council of Norway is also acknowledged for the support to the Norwegian Micro- and Nano-Fabrication Facility, NorFab, project numbers 295864. I.C. and Z.F. acknowledge funding from the Hungarian national project TKP2021-NKTA-05, VEKOP-2.3.3-15-2016-00002 of the European Structural and Investment Funds and János Bolyai Research Scholarship of the Hungarian Academy of Sciences. Noémi Szász is acknowledged for the TEM samples preparation.

Conflict of Interest

The authors declare no conflict of interest.

Data Availability Statement

The data that support the findings of this study are available from the corresponding author upon reasonable request.

Keywords

diffuse reflectance, gallium oxide, phase transformations, photoluminescence, polymorphism

Received: May 15, 2024
Revised: July 30, 2024
Published online:

[1] J. Y. Tsao, S. Chowdhury, M. A. Hollis, D. Jena, N. M. Johnson, K. A. Jones, R. J. Kaplar, S. Rajan, C. G. Van de Walle, E. Bellotti, C. L. Chua, R. Collazo, M. E. Coltrin, J. A. Cooper, K. R. Evans, S. Graham, T. A. Grotjohn, E. R. Heller, M. Higashiwaki, M. S. Islam, P. W. Juodawlkis, M. A. Khan, A. D. Koehler, J. H. Leach, U. K. Mishra, R. J. Nemanich, R. C. N. Pilawa-Podgurski, J. B. Shealy, Z. Sitar, M. J. Tadjer, et al., *Adv. Electron. Mater.* **2018**, *4*, 1600501.
[2] S. J. Pearton, J. Yang, P. H. Cary, F. Ren, J. Kim, M. J. Tadjer, M. A. Mastro, *Appl. Phys. Rev.* **2018**, *5*, 011301.
[3] M. J. Tadjer, *Science* **2022**, *378*, 724 .
[4] X. Chen, F. Ren, S. Gu, J. Ye, *Photonics Res.* **2019**, *7*, 381.
[5] R. Zhu, H. Liang, S. Liu, Y. Yuan, X. Wang, F. C.-C. Ling, A. Kuznetsov, G. Zhang, Z. Mei, *Nat. Commun.* **2023**, *14*, 5396.
[6] H. Y. Playford, A. C. Hannon, E. R. Barney, R. I. Walton, *Chem.-A Eur. J.* **2013**, *19*, 2803.
[7] I. Cora, F. Mezzadri, F. Boschi, M. Bosi, M. Caplovicova, G. Calestani, I. Dodony, B. Pecz, R. Fornari, *Cryst. Eng. Comm.* **2017**, *19*, 1509.
[8] T. Kato, H. Nishinaka, K. Shimazoe, K. Kanegae, M. Yoshimoto, *ACS Appl. Electron. Mater.* **2023**, *5*, 1715.
[9] L. Li, W. Wei, M. Behrens, *Solid State Sci.* **2012**, *14*, 971.
[10] D. Gentili, M. Gazzano, M. Melucci, D. Jones, M. Cavallini, *Chem. Soc. Rev.* **2019**, *48*, 2502.
[11] T. Yoo, X. Xia, F. Ren, A. Jacobs, M. J. Tadjer, S. Pearton, H. Kim, *Appl. Phys. Lett.* **2022**, *121*, 072111.
[12] H.-L. Huang, C. Chae, J. M. Johnson, A. Senckowski, S. Sharma, U. Singisetti, M. H. Wong, J. Hwang, *APL Mater.* **2023**, *11*, 061113.
[13] A. Azarov, J. García Fernández, J. Zhao, F. Djurabekova, H. He, R. He, Ø. Prytz, L. Vines, U. Bektas, P. Chekhonin, N. Klingner, G. Hlawacek, A. Kuznetsov, *Nat. Commun.* **2023**, *14*, 4855.
[14] J. Zhao, J. García-Fernández, A. Azarov, R. He, Ø. Prytz, K. Nordlund, M. Hua, F. Djurabekova, A. Kuznetsov, *arXiv*, **2024**, 2401.07675, https://arxiv.org/abs/2401.07675.
[15] A. Y. Polyakov, A. A. Vasilev, A. I. Kochkova, I. V. Shchemerov, E. B. Yakimov, A. V. Miakonkikh, A. V. Chernykh, P. B. Lagov, Y. S. Pavlov, A. S. Doroshkevich, R. Sh. Isaev, A. A. Romanov, L. A. Alexanyan, N. Matros, A. Azarov, A. Kuznetsov, S. Pearton, *J. Mat. Chem. C* **2024**, *12*, 1020.
[16] C. Wouters, M. Nofal, P. Mazzolini, J. Zhang, T. Remmele, A. Kwasniewski, O. Bierwagen, M. Albrecht, *APL Mater.* **2024**, *12*, 011110.
[17] S. B. Kjeldby, A. Azarov, P. D. Nguyen, V. Venkatachalapathy, R. Mikšová, A. Macková, A. Kuznetsov, Ø. Prytz, L. Vines, *J. Appl. Phys.* **2022**, *131*, 125701.
[18] J. García-Fernández, S. B. Kjeldby, L. Zeng, A. Azarov, A. Pokle, P. D. Nguyen, E. Olsson, L. Vines, A. Kuznetsov, Ø. Prytz, *Mater. Adv.* **2024**, *5*, 3824.
[19] K. Jiang, J. Tang, C. Xu, K. Xiao, R. F. Davis, L. M. Porter, *J. Vac. Sci. Technol. A* **2023**, *41*, 062702.
[20] J. Tang, K. Jiang, P. Tseng, R. C. Kurchin, L. M. Porter, R. F. Davis, *arXiv*, **2024**, 2405.00299, https://doi.org/10.48550/arXiv.2405.00299.
[21] A. F. M. Anhar Uddin Bhuiyan, Z. Feng, J. M. Johnson, H.-L. Huang, J. Sarker, M. Zhu, M. R. Karim, B. Mazumder, J. Hwang, H. Zhao, *APL Mater.* **2020**, *8*, 031104.
[22] J. F. Ziegler, M. D. Ziegler, J. P. Biersack, *Nucl. Instrum. Meth. B* **2010**, *268*, 1818.
[23] Powder diffraction file PDF #01-087-1901.
[24] Q.-S. Huang, X. Cai, X. Zhang, A. Kuznetsov, S.-H. Wei, *Phys. Rev. B* **2024**, *109*, 224105.
[25] F. Ricci, F. Boschi, A. Baraldi, A. Filippetti, M. Higashiwaki, A. Kuramata, V. Fiorentini, R. Fornari, *J. Phys.: Condens. Matter.* **2016**, *28*, 224005.
[26] A. Azarov, A. Galeckas, E. Wendler, E. Monakhov, A. Kuznetsov, *Appl. Phys. Lett.* **2024**, *124*, 042106.
[27] J. E. Stehr, M. Jansson, D. M. Hofmann, J. Kim, S. J. Pearton, W. M. Chen, I. A. Buyanova, *Appl. Phys. Lett.* **2021**, *119*, 052101.
[28] M. L. Myrick, M. N. Simcock, M. Baranowski, H. Brooke, S. L. Morgan, J. N. Mc Cutcheon, *Appl. Spectroscopy Rev.* **2011**, *46*, 140.
[29] Y. Wang, P. T. Dickens, J. B. Varley, X. Ni, E. Lotubai, S. Sprawls, F. Liu, V. Lordi, S. Krishnamoorthy, S. Blair, K. G. Lynn, M. Scarpulla, B. Sensale-Rodriguez, *Sci. Rep.* **2018**, *8*, 18075.

© 2024 The Author(s). Advanced Optical Materials published by Wiley-VCH GmbH

21951071, 0, Downloaded from https://onlinelibrary.wiley.com/doi/10.1002/adom.202401325 by Hun-Ren Centre For Energy Research, Wiley Online Library on [08/09/2024]. See the Terms and Conditions (https://onlinelibrary.wiley.com/terms-and-conditions) on Wiley Online Library for rules of use; OA articles are governed by the applicable Creative Commons License